Journal of Chromatography A, 1284 (2013) 148–154

Contents lists available at SciVerse ScienceDirect

Journal of Chromatography A

journal homepage: www.elsevier.com/locate/chroma

Rapid freezing cryo-polymerization and microchannel liquid-flow focusing for cryogel beads: Adsorbent preparation and characterization of supermacroporous bead-packed bed

Junxian Yun[a,b], Julian T. Dafoe[a], Eric Peterson[a], Linhong Xu[c], Shan-Jing Yao[d,**], Andrew J. Daugulis[a,*]

[a] Department of Chemical Engineering, Queen's University, Dupuis Hall, 19 Division Street, Kingston K7L3N6, Ontario, Canada
[b] State Key Laboratory Breeding Base of Green Chemistry Synthesis Technology, College of Chemical Engineering and Materials Science, Zhejiang University of Technology, Chaowang Road 18, Hangzhou 310032, China
[c] Faculty of Mechanical & Electronic Information, China University of Geosciences (Wuhan), Wuhan 430074, China
[d] Department of Chemical and Biological Engineering, Zhejiang University, Zheda Road 38, Hangzhou 310027, China

ARTICLE INFO

Article history:
Received 18 December 2012
Received in revised form 28 January 2013
Accepted 5 February 2013
Available online 11 February 2013

Keywords:
Cryogel bead
Supermacroporous bed
Anion-exchange adsorption
Protein
Microchannel

ABSTRACT

Cryogel beads, fabricated by the microchannel liquid-flow focusing and cryo-polymerization method, have micron-scale supermacropores allowing the passage of crude feedstocks, and could be of interest as chromatographic adsorbents in bioseparation applications. In this work, we provide a rapid freezing and continuous formation method for cryogel beads by cryo-polymerization using dry ice particles as the freezing source and microchannel liquid-flow focusing using peristaltic pumps for the fluid supply. Polyacrylamide (pAAm)-based supermacroporous cryogel beads were prepared and grafted with *N*,*N*-dimethylaminoethyl methacrylate (DMAEMA), which provided the anion-exchange cryogel beads with tertiary amine functional groups suitable for binding proteins. Properties of the supermacroporous cryogel-bead packed bed, i.e., permeability, bed voidage, protein breakthrough as well as protein adsorption performance by using bovine γ-globulin as model protein, were experimentally investigated. A capillary-based model was employed to characterize the supermacroporous bed performance, and gave a reasonable description of the microstructure and thus an insight into the flow, dispersion and mass transfer behaviors within the cryogel bead-packed bed. The results also showed that by using dry ice as the freezing source, it is easy to reduce the temperature below −55 to −61 °C in the bulk solution, causing the rapid formation of ice crystals within the monomer drops, and finally effective cryo-polymerization to form supermacropores within the cryogel beads. By using peristaltic pumps, continuous preparation was achieved and the obtained cryogel beads had favorable properties similar to those prepared using syringe pumps in the microchannel liquid-flow focusing process. This method is thus expected to be interesting in the liter- or even larger-scale preparation of cryogel adsorbents.

1. Introduction

Cryogels are sponge-like materials possessing supermacropores with sizes ranging from several to hundreds of microns [1–5]. This interesting class of porous materials has potential applications in biotechnology [6–9], tissue engineering [10–14], and drug delivery areas [15]. In the past several years, various monolithic cryogels for chromatographic separation of biomolecules have been prepared by the cryo-polymerization method and their properties and applications have been investigated by numerous researchers [1–5,16–32]. However, there are few reports on particle-based cryogels or cryogel beads for bioseparation applications due to a number of preparation difficulties such as controlling the bead size, the use of relatively complex equipment and scaling-up the preparation process. Recently, a new method that combines microchannel liquid-flow focusing with cryo-polymerization for the preparation of cryogel beads was proposed [33]. This method involves the formation of aqueous drops containing gel-forming agents using immiscible fluids via flow-focusing in a microchannel system, followed by *in situ* freezing to form solid-state cryo-polymerized particles, and finally thawing to form the cryogel beads. By this method it is possible to produce cryogel beads with a relatively narrow size distribution. After grafting functional groups onto the bead matrices, the cryogel beads packed in columns can be used to separate biomolecules from different feedstocks [33,34].

* Corresponding author. Tel.: +1 613 533 2784; fax: +1 613 533 6637.
** Corresponding author. Tel.: +86 571 87951982; fax: +86 571 87951982.
E-mail addresses: yaosj@zju.edu.cn (S.-J. Yao), andrew.daugulis@chee.queensu.ca (A.J. Daugulis).

0021-9673/$ – see front matter © 2013 Elsevier B.V. All rights reserved.
http://dx.doi.org/10.1016/j.chroma.2013.02.014

Notwithstanding such previous success, there are two limitations requiring improvement in the previous procedure of microchannel liquid-flow focusing and cryo-polymerization [33,34]. One is that drop formation and the flow focusing process are intermittent due to the batch operation of the syringe pumps, and the other is that the freezing process is slow. In the former situation, syringe pumps have been employed to inject the aqueous gel-forming solution and the water-immiscible phase solution simultaneously during liquid flow focusing, requiring that the pumps be stopped to draw fresh liquids into the syringes at about 6–10 min intervals. This requires continuous operator intervention and would also likely be difficult to use in large-scale preparation. In addition the flow focusing is also not stable over the course of the intervals, which can influence the drop sizes and thus the bead sizes. In the latter case the freezing process has not been sufficiently rapid because the temperature was always kept at about −26 to −23 °C. When the drop concentration was high, some aqueous drops could aggregate together before being frozen during mechanical stirring in the bulk phase, which could induce variations in the bead size distribution.

In this work, we describe stable and continuous microchannel flow-focusing by peristaltic pump, and a rapid freezing approach suitable for scale-up preparation by using dry ice for cryo-polymerization. pAAm-based anion-exchange cryogel beads were prepared using this method followed by graft polymerization with DMAEMA. The performance of a supermacroporous packed bed with these cryogel beads was determined and the breakthrough and adsorption performance of bovine γ-globulin was investigated. A model was also developed to characterize the bed performance.

2. Materials and methods

2.1. Materials

N,*N*′-Methylene-bis-acrylamide (MBAAm, 99%), DMAEMA (98%), ammonium persulfate (APS), *N*,*N*,*N*′,*N*′-tetramethylethylenediamine (TEMED, 99%), ethyl heptanoate (98%), and bovine γ-globulin were bought from Sigma–Aldrich. Acrylamide (AAm, 99.9%) was from Biobasic (Toronto, Canada) and Span 80 was from Fisher Scientific (USA). Other chemicals used (analytical grade) were obtained from local sources. All reagents were used as received.

2.2. Preparation of cryogel beads

The pAAm cryogel matrix beads were prepared in a stainless steel microchannel device from Wuhan Redywoods Bioengineering Co. Ltd. (Wuhan, China), and were similar to that used in our previous work [33,34]. The main microchannel has a width of 760 μm, depth of 606 μm and length of 50 mm, as schematically shown in Fig. 1. The branch channels with the same width and depth and 20 mm length each are located at a downstream position 20 mm from the inlet of the main channel. The cover seal slab was a polypropylene plate with thickness of about 2 mm.

Typically, the rapid freezing bath was prepared by adding about 1.8 L ethanol into a glass beaker, which was surrounded with about 3 kg dry ice particles in a styrofoam chamber, as shown in Fig. 1. Then, 300 mL water-immiscible solution (ethyl heptanoate containing 0.5% (v/v) Span 80 and 0.75 mg/mL TEMED) were added into a 1-L glass beaker, stirred mechanically at about 50–75 rpm and cooled to about −61 to −55 °C in the ethanol bath. The aqueous gel-forming solution contained AAm of 7.33% (w/w), MBAAm of 1.67% (w/w), TEMED and APS with the mass ratios to the total mass of AAm and MBAAm of 0.5% (w/w) and 1.2% (w/w) respectively. The aqueous phase (pre-cooled to about 2–4 °C) and the water-immiscible phase were pumped into the microchannel simultaneously with two peristaltic pumps (Masterflex C/L Dual-channel, Cole-Parmer, USA) at given flow rates for flow focusing, similar to our previous work [33]. The aqueous phase velocity U_{aq} was 1.3 ± 0.1 cm/s and the total velocity of the water-immiscible phase U_{im} was 6.5 ± 0.3 cm/s. The mixture suspension containing aqueous drops leaving the microchannel was introduced into the glass beaker containing water-immiscible solution and was frozen rapidly. The frozen beads were then filtered, kept at about −20 to −23 °C for 48 h, thawed at room temperature and washed with a dilute acetic acid solution and deionized water for further use. During the preparation process, the aqueous solution fractions were replaced with fresh solutions at the intake of the peristaltic pump for the aqueous liquid every 10 min in order to prevent polymerization of monomers within the microchannel thereby allowing us to achieve continuous preparation.

The obtained cryogel beads were grafted with DMAEMA using Cu(III) solution as the initiator [26,35]. Typically, about 8 mL beads were packed in a glass column with inner diameter of 10 mm and about 1 L deionized water with temperature of 45 °C was pumped thorough the bed. Then 20 mL 0.056 M Cu(III) solution and 10 mL 1 M NaOH solution with the same temperature were mixed and pumped through the column at a flow rate of 3 mL/min. After 40 min, 14 mL 1.5 M DMAEMA solution was pumped through the column and maintained for graft polymerization at the same velocity and temperature for another 2 h. The anion exchange cryogel beads were obtained by washing the column with 0.1 M HCl and deionized water. The maximum bead porosity φ_{max} and the effective bead porosity φ_e of the obtained anion exchange cryogel beads were measured according to the method reported previously [33].

2.3. Protein breakthrough and chromatographic adsorption in the cryogel bead packed bed

γ-Globulin was used as model protein. A supermacroporous bed with height of 82 mm for chromatographic breakthrough and adsorption of protein was prepared by packing 8.9 g wet anion exchange cryogel beads into a glass column with inner diameter of 10 mm. The water permeability k of the packed bed was determined by measuring the flow rates Q at different pressure drops based on Darcy's equation [25,31–33]. The binding and non-binding breakthrough curves of protein in the cryogel-bead bed were measured at various flow velocities. For the protein non-binding breakthrough, 1 mg/mL γ-globulin salt solution in 1 M NaCl and 50 mM (NaH_2PO_4/Na_2HPO_4) buffer (PBS, pH 7.6) were prepared and the breakthrough curves at various flow rates were measured by pumping 30 mL γ-globulin salt solution each through the bed. For the protein binding test, the column was equilibrated with 50 mM PBS (pH 7.6) and then 40 mL 1 mg/mL γ-globulin solution in 50 mM PBS (pH 7.6) was loaded. The column was washed with 40 mL PBS buffer, eluted with 28 mL 2 M NaCl in 50 mM PBS buffer and re-equilibrated with PBS buffer for the next run. The column effluent was collected as 2 mL fractions and the protein concentration in each fraction was determined by UV spectrometry (Ultrospec 3000, GE Healthcare) at 280 nm.

3. Results and discussion

3.1. Rapid-freezing cryo-polymerization and microchannel flow-focusing for cryogel beads

When the aqueous gel-forming solution and the water-immiscible solution were pumped into the microchannel, the liquid focusing of these immiscible flow streams occurred at the tee cross-junction. Consequently, liquid–liquid slug flow characterized by the

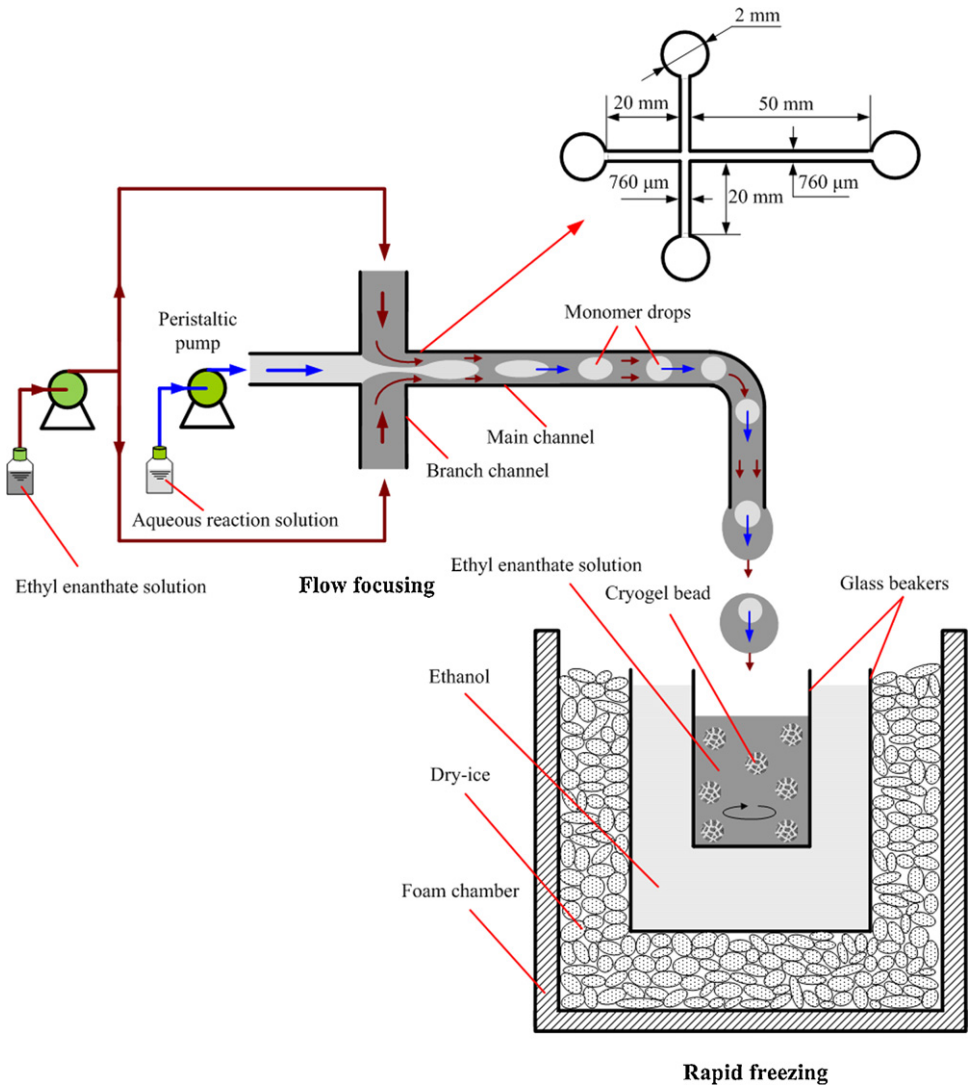

Fig. 1. Schematic diagram of the rapid freezing cryo-polymerization and microchannel liquid-flow focusing for cryogel beads.

aqueous drops being segmented by the water-immiscible slugs was observed. The motion of the liquid–liquid slug flow was not steady, but had an oscillatory and intermittent manner, i.e., it moved forward a distance, flowed back and then forward again, along the main channel due to the operation of the peristaltic pumps. Sometimes the liquid carrying aqueous drops near the cross-junction was drawn back into the branch channels or the entrance section of the main channel due to the back-flow of the liquid streams, and re-focusing occurred. During this process, some broken or aggregate aqueous drops were generated, which could cause a change in the bead sizes.

When the mixture suspension of water-immiscible solution and gel-forming aqueous drops generated in the main channel dripped into the cold water-immiscible bulk, the aqueous drops were frozen very rapidly (in about 1–3 s) to form frozen-state beads, because of the low temperature induced by the dry ice. The reactive gel-forming agents within these frozen-state beads were concentrated, and polymerized to form the skeleton of the cryogel beads, while the void spaces filled with ice crystals formed the supermacropores after thawing, similar to cryogel beads [33,34] and monolithic cryogels [1,2,4]. During the generation of frozen drops, the accelerator agent TEMED within the gel-forming aqueous drops could be extracted by the water-immiscible ethyl heptanoate, which could cause a decrease of the accelerator concentration and consequently result in poor polymerization of the bead matrices. Therefore, in this work, we added about 0.75 mg/mL TEMED into the water-immiscible fluid to maintain the concentration of TEMED within the gel-forming aqueous drops.

Fig. 2(a) shows an example of cryogel beads generated by the present method prepared at U_{aq} of 1.3 ± 0.1 cm/s and U_{im} of 6.5 ± 0.3 cm/s. The particle size distribution of these cryogel beads was estimated statistically by image measuring the diameters of about 200 beads randomly from Fig. 2(a). As can be seen, the diameters of these cryogel beads were in the range from about 500 to 2000 μm and the mean diameter was about 1110 μm, which are similar to beads with mean diameter values of 1091–1248 μm prepared at U_{aq} of 0.5–2.0 cm/s and U_{im} of 2.0–6.0 cm/s using syringe pumps and frozen at about −26 °C [33]. We also observed that the dried beads restored their original shapes rapidly after being immersed into water. Although the bead sizes were not as uniform as those prepared using syringe pumps [33,34], the present beads have acceptable, nearly spherical shapes and very similar sponge-like porous structures, including the pore sizes and the gel skeleton, similar to those prepared using syringe pumps reported in our previous work [33,34]. The maximum porosity φ_{max} of the cryogel beads prepared using the present method was 95.7% and the effective bead porosity φ_e was 85.6%, which were also very similar to the cryogel beads prepared previously [33]. It should be noted that the

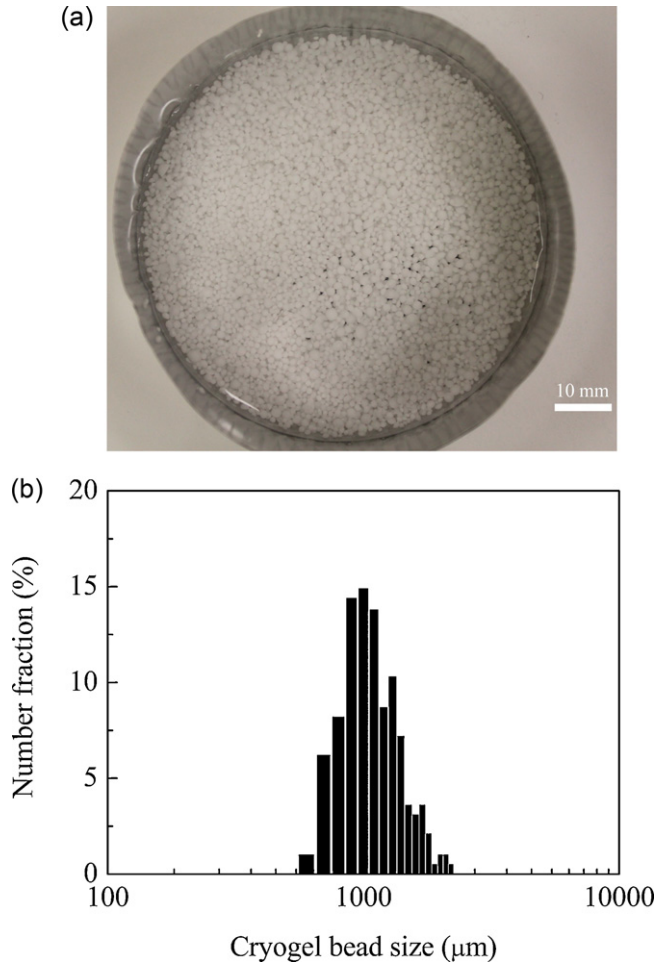

Fig. 2. Photograph (a) and particle size distribution (b) of the cryogel beads prepared at U_{aq} = 1.3 cm/s and U_{im} = 6.5 cm/s.

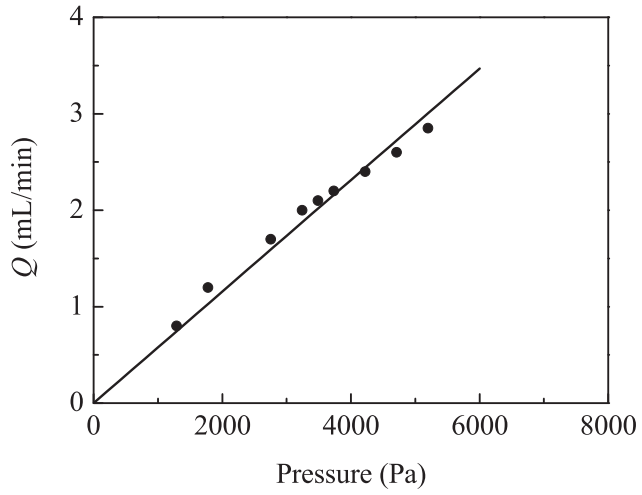

Fig. 3. Experimental (●) and fitted (—) flow rates as a function of pressure drop in the cryogel bead-packed bed.

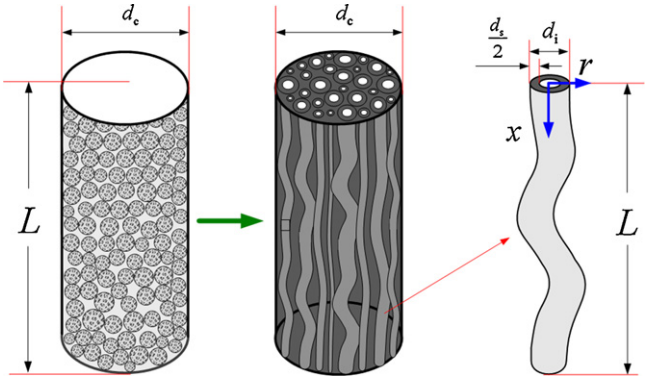

Fig. 4. Schematic diagram of the cryogel bead-packed bed with the bundle of tortuous capillaries as that for the monolithic cryogel.

present freezing process is advantageously much more rapid, and the preparation process is continuous. Due to the lower temperature here, the separation of the frozen beads from the bulk mixture was easier than in the previous preparation [33,34], because of the longer time before the frozen beads melted from being exposed to air during the separation operation. Therefore, this method is substantially more attractive in actual liter- or larger-scale preparation cases.

3.2. Characterization of the cryogel-bead packed bed

To evaluate the properties of the as-prepared cryogel beads in a bead-packed bed, the water permeability k was determined, and the non-binding breakthrough curves of γ-globulin, which was used as a protein tracer in the column, were also measured at superficial flow velocities of 1.92×10^{-4}, 3.61×10^{-4}, 6.53×10^{-4} and 9.88×10^{-4} m/s. Fig. 3 shows the obtained water flow rates at different pressure drops generated by the water columns. By fitting these experimental data with Darcy's equation, the obtained water permeability was 8.85×10^{-12} m^2. This value was close to those of monolithic cryogel beds [23,25,31,32], but lower than that of the cryogel bead-packed bed in reference [33]. In fact, the beads within the bed have a total free volume of 8.11 mL and the bed column has a volume of 6.44 mL. Therefore, after being packed into the column the beads were compressed and a tightly packed bed was obtained. By taking into account the bead porosity of 85.6%, the bed voidage was actually 81.9%, which was also lower than that reported previously [33] and consequently resulted in low water permeability.

To get insights in the micro-structure characteristics and mass transfer behaviors in the cryogel bead-packed bed, a capillary-based model valid for cryogel monoliths [29,31,32] was used to characterize the bead-packed bed properties. In reality, the cryogel-bead packed bed has inter-bead voids and intra-bead supermacropores [33]. These pores are generally in the micron-scale range and thus the microstructure could be very similar to that of a cryogel monolith. Therefore, we assumed that the bed could be represented as a porous medium made up of capillaries with a size distribution, as shown in Fig. 4. These capillaries are tortuous and have a normal size distribution the same as in reference [37]. The probability density function of capillary diameter distribution $f(d_i)$ is expressed as [31,32,37]

$$f(d_i) = \frac{1/(\sqrt{2\pi}\sigma)\exp[-(d_i - d_m)^2/(2\sigma^2)]}{1 - \int_{-\infty}^{d_{min}} 1/(\sqrt{2\pi}\sigma)\ \exp[-(d_i - d_m)^2/(2\sigma^2)]\ \delta d_i - \int_{d_{max}}^{+\infty} 1/(\sqrt{2\pi}\sigma)\ \exp[-(d_i - d_m)^2/(2\sigma^2)]\ \delta d_i} \quad (1)$$

where d_i is the diameter of the capillary i, d_m the mean diameter of capillaries in the cryogel-bead bed, σ the standard deviation of capillaries, d_{min} the minimum capillary diameter, and d_{max} the maximum capillary diameter, respectively. Each capillary has a tortuosity τ_i (for the ith capillary, which is a function of capillary diameter), thin skeleton thickness of $2d_s$ and a given diameter.

Equations for the probability density function of capillary diameter distribution, the porosity of the cryogel beads packed bed φ, the bed permeability, the relationship between the bed volume and the total volume of capillaries and skeleton walls, as well as the tortuosity are the same as those reported previously [31].

In the case of protein breakthrough without adsorption in the cryogel-bead packed bed, the mass balance equation in the mobile fluid phase of the tortuous capillary i is written as [29,31,32]

$$\frac{\partial C_{D\ i}(x_D, t_{D\ i})}{\partial t_{D\ i}} = \frac{1}{Pe_i}\frac{\partial^2 C_{D\ i}(x_D, t_{D\ i})}{\partial x_D^2} - \frac{\partial C_{D\ i}(x_D, t_{D\ i})}{\partial x_D} \quad (2)$$

where $C_{D\,i}$ is the dimensionless bulk-phase concentration of protein in the capillary i, x_D the dimensionless distance from the inlet along the capillary length, $t_{D\,i}$ the dimensionless time, and Pe_i the axial Peclet number, respectively. These dimensionless variables were defined as $C_{D\,i} = C_i/C_0$, $x_D = x/\tau_i L$, $t_{D\,i} = tU_i/\tau_i L$ and $Pe_i = \tau_i L U_i/D_{axi}$, with $\tau_i = L_i/L$ and $U_i = U_L d_i^2/32k\tau_i$. In these equations, x is the distance, t the time, L the bed height, C_0 the inlet concentration and U_L the superficial liquid flow velocity in the cryogel bed, while C_i is the bulk-phase concentration, U_i the velocity, L_i the length, and D_{axi} the axial liquid dispersion coefficient in the capillary i, respectively.

The tortuosity is described using a linear function of capillary diameter [29,31,32]

$$\tau_i = \tau_{d\ \min} + \frac{(d_i - d_{\min})}{(d_{\max} - d_{\min})}\left(\sqrt{\frac{t_{d\ \max} U_L}{32kL}}d_{\max} - \tau_{d\ \min}\right) \quad (3)$$

where $\tau_{d\,\min}$ is the tortuosity of the capillary with diameter $d_{\min}$ and $t_{d\,\max}$ the time for the tracer passing through the capillary with the diameter $d_{\max}$, respectively.

The axial dispersion coefficient D_{axi} in the tortuous capillary is given by the following expression [31,32] based on the correlation suggested by Gutsche and Bunke [36]

$$D_{axi} = \frac{D_{AB}}{\tau_i} + \frac{1}{0.018\ \ Pe_{AB\ i}^{0.775}}\frac{U_i^2 d_i^2}{192\ \ D_{AB}} \quad (4)$$

where the molecule Peclet number in capillary i is $Pe_{AB\ i} = d_i U_i/D_{AB}$ and D_{AB} is the molecular diffusion coefficient of protein.

The effluent protein concentration C during the breakthrough process is then calculated based on the flow rates in each capillary Q_i and the total flow rate Q [31].

$$C = \frac{\sum_i^{N_g} C_i n_i Q_i}{Q} \quad (5)$$

Other equations and the initial and boundary conditions included in the model were the same as those in reference [31]. The model was solved numerically using a finite difference method [31,32]. In the calculation, the density of the γ-globulin solution was 1038 kg/m^3 and the viscosity was estimated by the formula reported by Monkos and Turczynski [38], which gave a value of 1.04 mPa s in the non-binding breakthrough test. The molecular diffusion coefficient of γ-globulin was calculated using the equation proposed by Young et al. [39] and the value was found to be 4.42×10^{-11} m^2/s. By fitting the model with the experimental values of the bed voidage, the water permeability and the breakthrough data, we obtained a bed voidage of 84.3% and a water permeability of 8.61×10^{-12} m^2, which are all close to the above experimental values. The total number of capillaries is 12603 and the obtained parameters of the microstructure are $d_{\min} = 3$ μm, $d_{\max} = 265$ μm, $d_m = 25$ μm, $\sigma = 30$ μm and the half thickness of the skeleton wall $d_s = 4.3$ μm.

Fig. 5 shows the matched pore size distribution in the cryogel bead-bed. As can be seen, the effective capillary diameters are in the range of 3–130 μm, while the contribution of capillaries with $d_i < 2$ μm and $d_i > 130$ μm has been neglected. Compared with

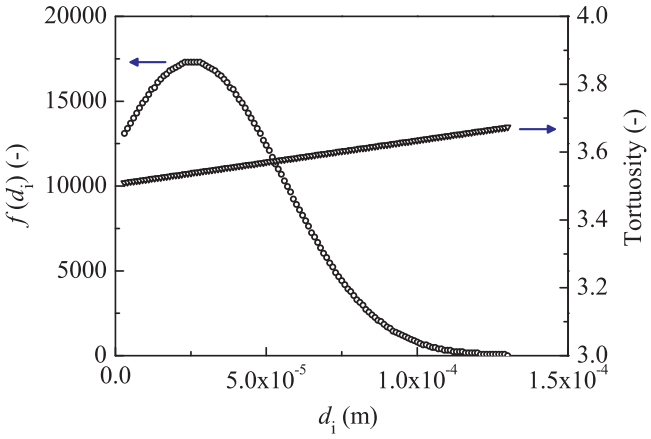

Fig. 5. Tortuosities and capillary diameter distribution in the model.

monolith cryogels [31,32], the pore sizes of the bead-packed bed are slightly wider. It is also seen that the variation of the tortuosity with the capillary diameter is not significant because the tortuosities increased only slightly, from 3.51 to 3.67 with an increase in the capillary diameter from 3 to 130 μm. This is due to the tight packing of some compressed inter-bead voids in the packed bed, which could have comparable sizes to the intra-bead supermacropores within the beads, and thus could also contribute to the formation of pores with narrow tortuosities for fluid flow. Those small pores within the beads could be more tortuous, while the large pores could tend to be more uniform than those in monolith cryogels [31,32].

Fig. 6 shows the variation of the axial dispersion coefficients of γ-globulin in capillaries with superficial liquid flow velocity. It is seen that the axial dispersion coefficients increased with an increase of both the capillary diameter and the superficial liquid velocity. These values were in the range of 10^{-11}–10^{-5} m^2/s, similar to the values measured previously [33]. The mean axial dispersion coefficients calculated by the model, using the same equations in [31], were 1.84×10^{-7}, 3.98×10^{-7}, 8.24×10^{-7} and 1.37×10^{-6} m^2/s at superficial liquid velocities of 1.92×10^{-4}, 3.61×10^{-4}, 6.53×10^{-4}, and 9.88×10^{-4} m/s, respectively. These values are slightly higher than those of lysozyme and bovine serum albumin in monolith cryogels [31]. The reason is that the wide

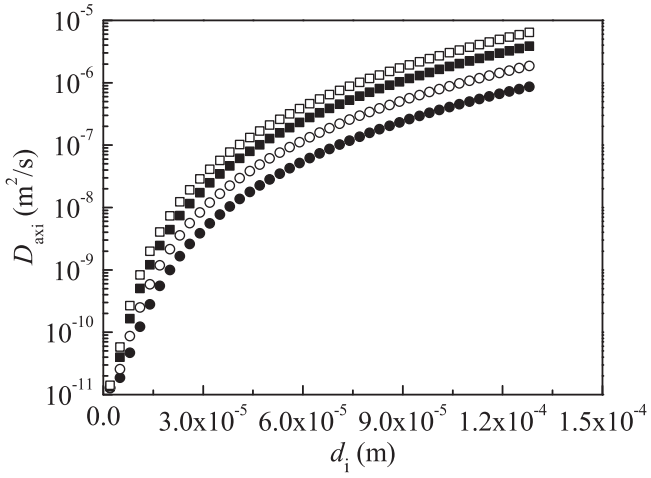

Fig. 6. Variation of axial dispersion coefficients with capillary diameter in the cryogel bead-packed bed at liquid flow velocities of 1.92×10^{-4} (●), 3.61×10^{-4} (○), 6.53×10^{-4} (■), and 9.88×10^{-4} m/s (□), respectively.

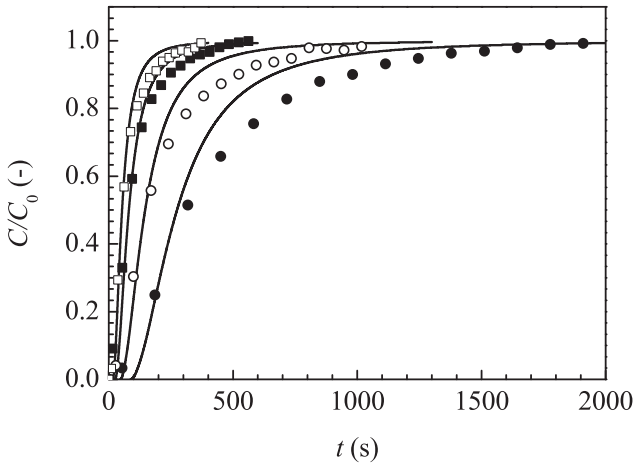

Fig. 7. Comparison of the fitted and experimental breakthrough curves of bovine γ-globulin in the cryogel bead-packed bed under non-binding condition at liquid flow velocities of 1.92×10^{-4} (●), 3.61×10^{-4} (○), 6.53×10^{-4} (■), and 9.88×10^{-4} m/s (□), respectively. The solid lines represent the calculation results by the model.

pore size distribution due to both the inter-bead voids and intra-bead supermacropores induced stronger dispersion in the present bead-bed than those in monolithic cryogels.

Fig. 7 shows the calculated and experimental breakthrough curves of γ-globulin without binding at liquid velocities of 1.92×10^{-4}, 3.61×10^{-4}, 6.53×10^{-4} and 9.88×10^{-4} m/s, respectively. In the figure, C is the concentration of γ-globulin in the effluent, C_0 the γ-globulin concentration in the load solution and t the time. As can be seen, the model gave a good description of the breakthrough curves compared with most of the experimental data and thus the obtained parameters regarding the microstructure of cryogel beads should be close to the actual values.

3.3. Chromatographic adsorption of γ-globulin through the cryogel-bead packed bed

The chromatographic adsorption of γ-globulin was tested at various velocities, and the obtained breakthrough, wash and elution performances are shown in Fig. 8. The maximum breakthrough concentration ratios at a loaded volume of 40 mL were about 68.0%, 67.9%, 70.3% and 72.9%, while the binding capacities from the elution peaks were 1.95, 2.10, 1.81 and 1.63 mg/ml bed at velocities of 1.57×10^{-4}, 3.23×10^{-4}, 6.56×10^{-4} and 9.28×10^{-4} m/s, respectively. The trend of the capacity varying with liquid flow velocity was similar to the cation-exchange cryogel beads, but the capacities of γ-globulin were higher than those of lysozyme [33]. The capacities of γ-globulin were similar to those of bovine serum albumin in anion-exchange monolith cryogels [24,26]. It is also seen that the breakthrough curves displayed a slow increasing behavior with an increase of loaded volume in the range from about 10–40 mL. The reason is that there is a wide pore size distribution in the bed, which could induce strong dispersion and thus the slow-rise breakthrough curves. The in-pore diffusion of proteins within those small pores could also be the limiting step of the mass transfer process, which requires a long time for the protein molecules diffusing from the bulk solution to the pore walls and adsorption sites.

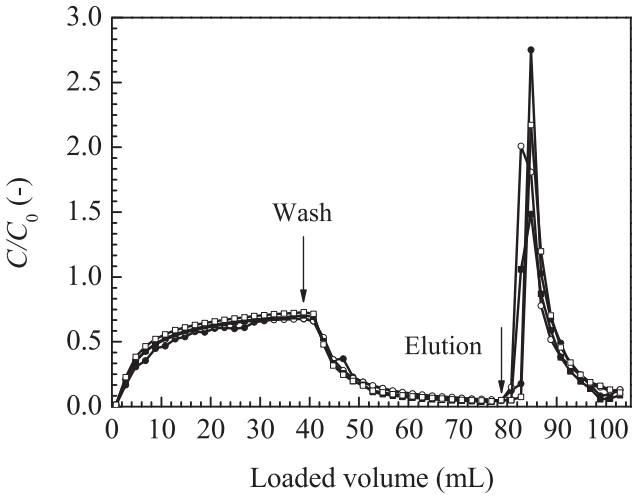

Fig. 8. Chromatographic profiles of bovine γ-globulin in the cryogel bead-packed bed at liquid flow velocities of 1.57×10^{-4} (●), 3.23×10^{-4} (○), 6.56×10^{-4} (■), and 9.28×10^{-4} m/s (□), respectively.

4. Conclusions

A rapid freezing method for the preparation of cryogel beads by cryo-polymerization and microchannel liquid-flow focusing was successfully demonstrated. By using dry ice as the freezing resource and peristaltic pumps for the fluid supply, the frozen beads can be formed very rapidly and continuous production can be readily achieved. The cryogel beads prepared by this method have acceptable properties regarding bead morphology, size and porosity. Therefore, this method is attractive in liter- or even larger-scale preparation.

By grafting on functional groups, the anion exchange cryogel beads are suitable to bind protein. A packed bed of these cryogel beads has reasonable voidage, permeability as well as protein breakthrough behavior and binding capacities. The microstructure, mass transfer and dispersion performance of the bead-packed bed can be characterized by the capillary-based model of monolith in cryogels and the related parameters can be estimated by matching the model with the experimental breakthrough curves. The chromatographic capacity of γ-globulin in the cryogel bead-packed bed is around 2 mg/ml bed even at high velocity and thus is expected to be useful in bioseparation applications.

Acknowledgments

This work was supported by the Natural Sciences and Engineering Research Council of Canada. The authors also gratefully acknowledge the financial supports partially by the National Natural Science Foundation of China (Nos. 21036005, 20876145, 20606031), the International Science & Technology Cooperation Program of China between China and Europe Country's Governments from the Ministry of Science and Technology (No. 1017 with S2010GR0616), the Visiting Scholar Foundation for "151 Talents project" from Zhejiang Province and the Zhejiang Provincial Natural Science Foundation of China.

References

[1] F.M. Plieva, H. Kirsebom, B. Mattiasson, J. Sep. Sci. 34 (2011) 2164.
[2] F.M. Plieva, I.Y. Galaev, W. Noppe, B. Mattiasson, Trends Microbiol. 16 (2008) 543.
[3] V.I. Lozinsky, Russ. Chem. Bull. 57 (2008) 1015.
[4] F.M. Plieva, I.Y. Galaev, B. Mattiasson, J. Sep. Sci. 30 (2007) 1657.
[5] V.I. Lozinsky, I.Y. Galaev, F.M. Plieva, I.N. Savina, H. Jungvid, B. Mattiasson, Trends Biotechnol. 21 (2003) 445.
[6] N.S. Bibi, P.R. Gavara, S.L.S. Espinosa, M. Grasselli, M. Fernández-Lahore, Biotechnol. Prog. 27 (2011) 1329.
[7] A. Hanora, F.M. Plieva, M. Hedström, I.Y. Galaev, B. Mattiasson, J. Biotechnol. 118 (2005) 421.
[8] E. Jain, A.A. Karande, A. Kumar, Biotechnol. Prog. 27 (2011) 170.
[9] E. Velickova, E. Winkelhausen, S. Kuzmanova, M. Cvetkovska, C. Tsvetanov, React. Funct. Polym. 69 (2009) 688.
[10] S. Bhat, A. Tripathi, A. Kumar, J. R. Soc. Interface 8 (2011) 540.

[11] K. Bloch, A. Vanichkin, L.G. Damshkaln, V.I. Lozinsky, P. Vardi, Acta Biomater. 6 (2010) 1200.
[12] M.B. Dainiak, I.U. Allan, I.N. Savina, L. Cornelio, E.S. James, S.L. James, S.V. Mikhalovsky, H. Jungvid, I.Y. Galaev, Biomaterials 31 (2010) 67.
[13] M. Jurga, M.B. Dainiak, A. Sarnowska, A. Jablonska, A. Tripathi, F.M. Plieva, I.N. Savina, L. Strojek, H. Jungvid, A. Kumar, B. Lukomska, K. Domanska-Janik, N. Forraz, C.P. McGuckin, Biomaterials 32 (2011) 3423.
[14] N. Kathuria, A. Tripathi, K.K. Kar, A. Kumar, Acta Biomater. 5 (2009) 406.
[15] B. Kostova, D. Momekova, P. Petrov, G. Momekov, N. Toncheva-Moncheva, C.B. Tsvetanov, N. Lambov, Polymer 52 (2011) 1217.
[16] H. Kirsebom, D. Topgaard, B. Mattiasson, I.Y. Galaev, Langmuir 26 (2010) 16129.
[17] H. Kirsebom, G. Rata, D. Topgaard, B. Mattiasson, I.Y. Galaev, Macromolecules 42 (2009) 5208.
[18] F.M. Plieva, E.D. Seta, I.Y. Galaev, B. Mattiasson, Sep. Purif. Technol. 65 (2009) 110.
[19] G. Baydemir, N. Bereli, M. Andaç, R. Say, I.Y. Galaev, A. Denizli, React. Funct. Polym. 69 (2009) 36.
[20] H. Kirsebom, G. Rata, D. Topgaard, B. Mattiasson, I.Y. Galaev, Polymer 49 (2008) 3855.
[21] F. Chen, K.J. Yao, J.X. Yun, S.C. Shen, Chem. Eng. Sci. 63 (2008) 71.
[22] R.V. Ivanov, V.I. Lozinsky, S.K. Noh, S.S. Han, W.S. Lyoo, J. Appl. Polym. Sci. 106 (2007) 1470.
[23] K.J. Yao, J.X. Yun, S.C. Shen, F. Chen, J. Chromatogr. A 1157 (2007) 246.
[24] I.N. Savina, I.Y. Galaev, B. Mattiasson, J. Mol. Recognit. 19 (2006) 313.
[25] K.J. Yao, J.X. Yun, S.C. Shen, L.H. Wang, X.J. He, X.M. Yu, J. Chromatogr. A 1109 (2006) 103.
[26] I.N. Savina, I.Y. Galaev, B. Mattiasson, J. Chromatogr. A 1092 (2005) 199.
[27] I.N. Savina, B. Mattiasson, I.Y. Galaev, Polymer 46 (2005) 9596.
[28] F.M. Plieva, I.N. Savina, S. Deraz, J. Andersson, I.Y. Galaev, B. Mattiasson, J. Chromatogr. B 807 (2004) 129.
[29] P. Persson, O. Baybak, F.M. Plieva, I.Y. Galaev, B. Mattiasson, B. Nilsson, A. Axelsson, Biotechnol. Bioeng. 88 (2004) 224.
[30] F. Yılmaz, N. Bereli, H. Yavuz, A. Denizli, Biochem. Eng. J. 43 (2009) 272.
[31] J.X. Yun, G.R. Jespersen, H. Kirsebom, P.-E. Gustavsson, B. Mattiasson, I.Y. Galaev, J. Chromatogr. A 1218 (2011) 5487.
[32] J.X. Yun, H. Kirsebom, I.Y. Galaev, B. Mattiasson, J. Sep. Sci. 32 (2009) 2601.
[33] J.X. Yun, C.M. Tu, D.-Q. Lin, L.H. Xu, Y.T. Guo, S.C. Shen, S.H. Zhang, K.J. Yao, Y.-X. Guan, S.-J. Yao, J. Chromatogr. A 1247 (2012) 81.
[34] W.P. Deng, G.H. Zhang, L.H. Xu, S.C. Shen, J.X. Yun, K.J. Yao, Preparation of poly(2-hydroxyethyl methacrylate) cryogel microbeads and the isolation of adenosine triphosphate from *Saccharomyces cerevisiae* broths thereafter, J. Chem. Eng. Chinese Univ. 27, in press (in Chinese).
[35] A. Hanora, I. Savina, F. Plieva, V.A. Izumrudov, B. Mattiasson, I.Y. Galaev, J. Biotechnol. 123 (2006) 343.
[36] R. Gutsche, G. Bunke, Chem. Eng. Sci. 63 (2008) 4203.
[37] J.X. Yun, D.Q. Lin, S.J. Yao, J. Chromatogr. A 1095 (2005) 16.
[38] K. Monkos, B. Turczynski, Int. J. Biol. Macromol. 26 (1999) 155.
[39] M.E. Young, P.A. Carroad, R.L. Bell, Biotechnol. Bioeng. 22 (1980) 947.